PHYSICAL REVIEW A VOLUME 24, NUMBER 5 NOVEMBER 1981

Structural correlations in smectic-*F* and smectic-*I* phases

P. A. C. Gane and A. J. Leadbetter
Chemistry Department, University of Exeter, Exeter EX4 4QD, United Kingdom

J. J. Benattar and F. Moussa
Laboratoire Leon Brillouin, Centre d'Etudes Nucléaires de Saclay, 91191 Gif-sur-Yvette Cedex, France

M. Lambert
Laboratoire de Physique des Solides, Université Paris-Sud, 91405 Orsay, France

(Received 21 May 1981)

The x-ray diffraction pattern from aligned samples of the smectic-*I* (Sm*I*) phases of a number of compounds has been considered, with particular emphasis on TBDA ($C_{10}H_{21}$ PhNCHPhCHNPh$C_{10}H_{21}$, where Ph stands for the phenyl group) which exhibits both Sm*I* and smectic-*F* (Sm*F*) phases. It is established that both Sm*I* and Sm*F* phases are quasi-two-dimensional structures, with essentially no correlation of molecular positions between layers. They each have C-centered monoclinic lattices with long-range three-dimensional order of the lattice directions (bond orientational order) but do not have long-range positional order. The Sm*F* and Sm*I* phases differ in the direction of molecular tilt relative to the hexagonal packing of the molecular long axes: In terms of the unit cell axes, with b the unique axis, $a > b$ for Sm*F* and $b > a$ for Sm*I*. Analysis of intensity profiles from high-resolution powder measurements has led to a quantitative description of the correlation function for the molecular positions in the smectic layers. The Sm*F* phase has exponential decay of correlation with correlation lengths of order 100 Å, while the (higher temperature) Sm*I* phases show algebraic decay as expected for a truly two-dimensional crystal. Current theories do not account for this result.

INTRODUCTION

Of the phases which have hitherto been classified as "smectics" it is now clear that a number (e.g., Sm*E*, Sm*G*, Sm*H*) are truly crystalline in the sense that they exhibit long-range 3D positional order of the molecules (although still possessing considerable orientational disorder). On the other hand, the Sm*A* and Sm*C* phases are true liquid crystals with 1D density waves either parallel to the director ($\hat{n}$ or z direction) for Sm*A* or at an angle (β_t) to it for Sm*C*. These density waves do not have long-range order but rather a correlation function with algebraic decay [$G(\vec{r}) \sim r^{-\eta}$] which results in a power-law singularity in the scattering of the form[1] (for Sm*A*) $S(\vec{q}) \sim q_z^{-2+\eta}(q_z \gg q_\perp) \sim q^{-4+\eta}(q \gg q_\perp)$.

There also exist at least three intermediate phases Sm*B*, Sm*F*, Sm*I* which may lack long-range 3D positional order.[2] There now appear to be two kinds of "Sm*B*" phase: "crystal *B*" which is a hexagonal crystal and a "hexatic *B*" which has only short-range hexagonal ordering of molecular positions but does have long-range bond orientational order.[3] The first phase of this latter type to be recognized was in fact the Sm*F* phase[4] and more recently the existence of the Sm*I* phase has also been established.[2,5] It is the purpose of this paper to determine the types of correlation existing in these two tilted phases.

THE NATURE OF Sm*F* AND Sm*I* PHASES

The Sm*F* and Sm*I* phases were first revealed as having distinct identities by means of miscibility and optical studies. Powder x-ray-diffraction photographs of Sm*B*, Sm*F*, and Sm*I* phases are qualitatively similar in showing only one "outer ring" corresponding to the first *hk*0 ring of the reciprocal lattice, although the width of this ring appeared in general to be sharper for Sm*B* and Sm*I* than for Sm*F*. X-ray diffraction studies[2,4,6,7] of aligned specimens of Sm*F* revealed a tilted structure with 3D long-range bond orientational order but only short-range ($\xi \sim 100$ Å) positional order within a layer and almost none between layers. The molecular packing is essentially hexagonal in the plane normal to the long axes [the short-range correlation makes it difficult to specify positively whether the (*hk*0) plane of the reciprocal lattice has exact hexagonal symmetry] and this gives a local structure which is C-centered monoclinic; the lattice axes having long-range order of *direction*. This was in fact the first experimental example of an hexatic type of phase which was predicted theoretically for 2D systems, although the Sm*F* is more properly described as a stacked tilted hexatic phase.

More recently,[2] similar measurements have been made on the Sm*I* phase and in particular an example was studied (TBDA see Table I) which exhi-

TABLE I. Examples of Sm*F* and Sm*I* phases characterized by x-ray diffraction.

Code	
TBPA	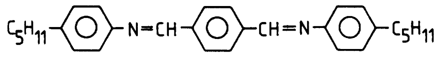 $\mathrm{Cr}\ -\ \mathrm{H} \xleftrightarrow{61} \mathrm{G} \xleftrightarrow{140} \mathrm{F} \xleftrightarrow{149} \mathrm{C} \xleftrightarrow{179} \mathrm{A} \xleftrightarrow{212} \mathrm{N} \xleftrightarrow{233} \mathrm{Iso}^{a,b}$ $\mathrm{Cr} \xrightarrow{68} \mathrm{G}$
TBDA	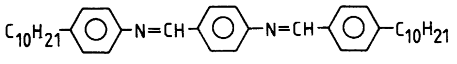 $\mathrm{Cr} \xrightarrow{73} \mathrm{G} \xleftrightarrow{120} \mathrm{F} \xleftrightarrow{150} \mathrm{I} \xleftrightarrow{156} \mathrm{C} \xleftrightarrow{191} \mathrm{A} \xleftrightarrow{192} \mathrm{Iso}$
PDOBAC	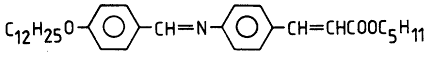 $\mathrm{Cr} \xrightarrow{78} \mathrm{I} \xleftrightarrow{95} \mathrm{C} \xleftrightarrow{107} \mathrm{A} \xleftrightarrow{137} \mathrm{Iso}$
HEPTOBPD†	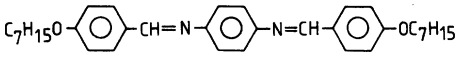 $\mathrm{Cr} \xrightarrow{146} \mathrm{H'} \xleftrightarrow{154} \mathrm{G'} \xleftrightarrow{157} \mathrm{I} \xleftrightarrow{164} \mathrm{C} \xleftrightarrow{197} \mathrm{N} \xleftrightarrow{241} \mathrm{Iso}$
8OSF	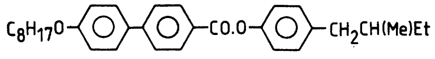 $\mathrm{Cr}\ -\ \mathrm{H'} \xleftrightarrow{61} \mathrm{G'} \xleftrightarrow{72} \mathrm{I} \xleftrightarrow{79} \mathrm{C} \xleftrightarrow{132} \mathrm{A} \xleftrightarrow{171} \mathrm{N} \xleftrightarrow{174} \mathrm{Iso}$ $\mathrm{Cr} \xrightarrow{76} \mathrm{I}$
HOBACPC	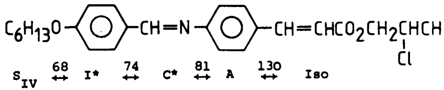 $\mathrm{Cr} \xrightarrow{60} \mathrm{S_{IV}} \xleftrightarrow{68} \mathrm{I^{*}} \xleftrightarrow{74} \mathrm{C^{*}} \xleftrightarrow{81} \mathrm{A} \xleftrightarrow{130} \mathrm{Iso}$ (Chiral)
50·6	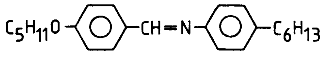 $\mathrm{Cr} \xrightarrow{36} \mathrm{G} \xleftrightarrow{38} \mathrm{F} \xleftrightarrow{42} \mathrm{B} \xleftrightarrow{50} \mathrm{C} \xleftrightarrow{52} \mathrm{A} \xleftrightarrow{60} \mathrm{N}$
90·4	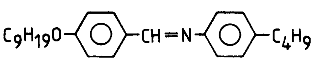 $\mathrm{Cr} \xrightarrow{48} \mathrm{G} \xleftrightarrow{67} \mathrm{F} \xleftrightarrow{69} \mathrm{A} \xleftrightarrow{82} \mathrm{Iso}$

[a] Cr, N, and Iso stand, respectively, for crystal, nematic, and isotropic liquid phases. The letters *A*, *B*, etc., denote the type of smectic phase and the numbers are transition temperatures in °C.

[b] *H'* and *G'* are phases analogous to *G* and *H* but with tilt direction similar to *I* rather than *F*[2].

bits both Sm*I* and Sm*F* phases. A similar structure was revealed, except that the tilt directions in the two phases are different and the correlation length in the Sm*I* is greater. In terms of the C-centered monoclinic cell, with *b* the unique axis, $a>b$ for Sm*F* and $b>a$ for Sm*I*; or, in terms of the hexagonal molecular packing the tilt is towards an edge of the hexagon in Sm*F* and towards an apex in Sm*I*. The transition presumably occurs by an azimuthal rotation of the molecules through $\pi/6$, with approximately constant tilt angle, as shown in Fig. 1(a). These results are illustrated in both real and reciprocal space in Fig. 1. The important points to note are the following: (a) the $00l$ reflections are of resolution-limited widths; (b) only the lowest-order $hk0$ reflections are observed and these have the shape of diffuse bars of scattering of length $\gtrsim \pm c^*$ which indicates immediately the restricted positional correlation within layers and very weak interlayer correlation; (c) no hkl reflections are observed; (d) the difference in tilt directions between Sm*F* and Sm*I* is revealed most directly by the symmetry of the diffraction patterns for the fiber-texture samples. Note also that the original papers[4,5] show that both for Sm*F* and Sm*I* the $hk0$ ring intensity has six maxima indicating the existence of long-range bond orientation, and high-resolution powder measurements (see below) show that the (020) and (110) planes have identical spacings for the Sm*I* phase indicating true hexagonal symmetry of the ($hk0$) reciprocal lattice plane and hence of the molecular packing.

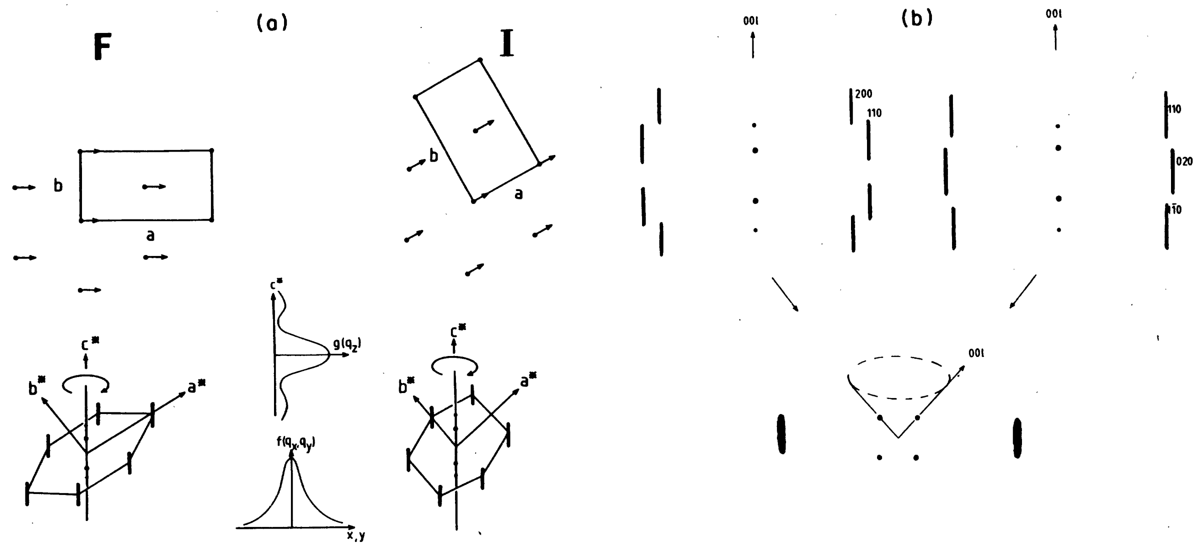

FIG. 1. (a) Schematic representations of real (upper) and reciprocal (lower) lattices for SmF and SmI phases. The arrows show the direction of tilt of the molecular long axes. Also shown are schematic intensity profiles of the diffuse bars of scattering, where $g(q_z)$ represents the profile parallel to c^* and $f(q_x, q_y)$ represents the profile in the a, b^* (or b) plane. (b) Diffraction patterns for SmF and SmI phases for fiber-aligned samples: upper pattern for sample disordered about c^* and lower disordered about c.

The C-centered monoclinic structure of the SmI phase with $b > a$ has been positively established for two compounds, TBDA and PDOBAC (defined in Table I), for which the existence of SmI had first been established by other means. For PDOBAC we have confirmed the results of Diele *et al.*[5] in our laboratory. We have also examined HEPTOBPD which was known to have a rich polymorphism and a preliminary study of which led Barrall *et al.*[8] to suggest that it exhibited an SmF phase. Our diffraction experiments[9] on a fiber-aligned sample showed an SmI-type structure ($b > a$) and subsequent optical reexamination and miscibility studies confirmed also an SmI.[9] Thus we have three separate examples, one also having an SmF phase, in which a particular tilt direction of the C-centered monoclinic cell ($b > a$) is associated with an SmI phase, and we conclude that this structure is characteristic of SmI and distinguishes SmI from SmF.

This leads to the reappraisal of previously published data to reveal further examples of SmI phases. Thus in the first paper,[4] which established the essential SmF structure, studies were made on fiber-oriented samples of TBPA and 8OSF (Table I) but it is now absolutely clear that while TBPA is indeed SmF, 8OSF is an SmI. Subsequent miscibility studies have now also confirmed this. It also now seems clear that the smectic-III phase of the ferroelectric liquid crystal HOBACPC and related compounds studied by Doucet *et al.*[10] has an SmI phase as it has precisely the characteristics described above.

Table I summarizes the phase behavior of those compounds which have now been positively identified as SmF and SmI by x-ray studies on aligned samples. Also included are two $nO \cdot m$ compounds which have been characterized as SmF by miscibility and microscopy but which x-ray studies have not *positively* confirmed as SmF. For $9O \cdot 4$ (Ref. 6) adequate sample alignment was not obtained but the intensity profile suggests that this could well be SmI. For $5O \cdot 6$ (Ref. 7) an alignment of the *molecules* was obtained rather than of the *layer normals*, see Fig. 1, so the direction of tilt was undetermined.

ANALYSIS OF THE QUASI-2D ORDER IN SmF AND SmI PHASES

Aligned samples

All measurements on aligned samples were low-resolution photographic experimental but nevertheless gave important results. In the first place they give the different directions of tilt for the two phases. Second, they show that the scattering centered on the ±1, ±1, 0 and ±2, 0, 0 or 0, ±2, 0 reciprocal lattice points is in the form of diffuse elongated bars. Profiles of these are shown in Figs. 2 and 3 for both phases of TBDA and for the SmI phase of PDOBAC. The profile of the bars in the $\langle 00l \rangle$ directions is similar in shape to the molecular structure factor but even more diffuse. This indicates that the effective correlation length between layers is less than one layer. Chain melt-

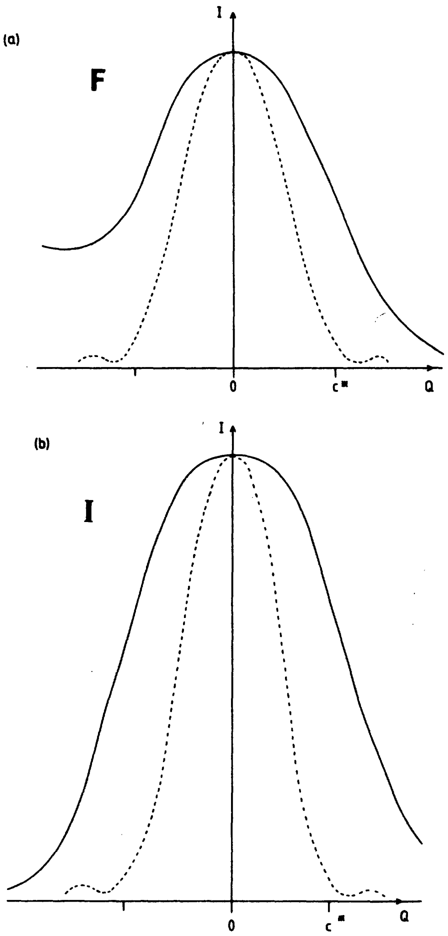

FIG. 2. Intensity profiles parallel to c^* of (a) the 110 scattering bar of the SmF phase of TBDA and (b) the 020 scattering bar of the SmI phase. Solid lines: experimental results; dashed lines: molecular structure factor $\langle F_m(z)\rangle^2$.

ing and sample mosaicity may contribute to this effect, especially through surface alignment producing a spread of $\langle 00l\rangle$ directions out of the plane of the paper in Fig. 1(b), but we cannot account for it quantitatively. The profiles perpendicular to the c^* axis are compared for the two phases in Fig. 3. For SmF a Lorentzian broadening describes the profile well and indicates a correlation length of $\xi \geq 50$ Å. The half-width of the scattering for SmI is narrower ($\xi \gtrsim 180$ Å) but there is extra scattering in the wings, showing that the mathematical form of the scattering is different. However, it is not worthwhile attempting a detailed analysis given the present resolution and accuracy. Furthermore, the width of the profiles is sample dependent and has shown variation of more than a factor of 3 between samples, though for each sample, the correlation length is consistently shorter in SmF than in SmI. Also, for both

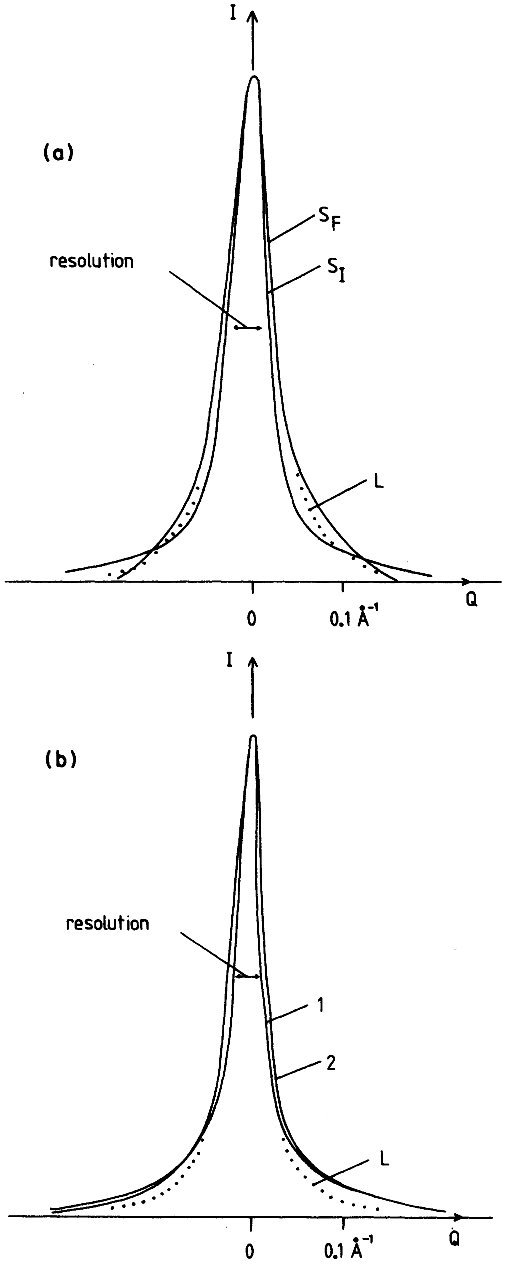

FIG. 3. (a) Experimental intensity profiles perpendicular to c^* of the 110 scattering bar for SmF and 020 scattering bar for SmI of TBDA. The dotted line shows the best fit Lorentzian for the SmF profile. (b) Intensity profiles perpendicular to c^* for the SmI phases of (1) PDOBAC and (2) TBDA. The dotted line shows the best-fit Lorentzian for the TBDA data. Note the broader wings in the SmI data compared with SmF and Lorentzian curves.

SmF and SmI the magnitudes of the widths are much greater than those inferred from analysis of powder diffraction profiles (see below). This suggests that preparation of an aligned sample by slow cooling, under the constraint of a magnetic field and surfaces, from isotropic liquid via the intermediate phases may reduce the correlation length compared with that obtained in forming a powder through unconstrained transitions from crystal or isotropic liquid. Nevertheless, the results on aligned samples confirm the structural description given earlier and show the phases to have 3D bond orientational order, positionally uncorrelated layers with no long-range order in the layers. Detailed quantitative analysis of the correlation in the layers has therefore been made on powder samples because reproducible (intrinsic) correlations are obtained and high experimental resolution was available.

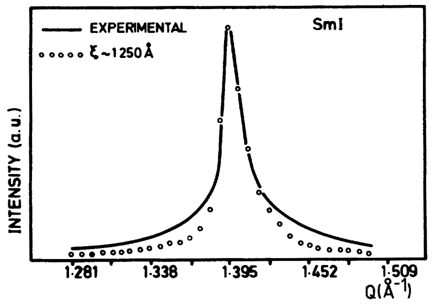

FIG. 5. Calculation showing that a Lorentzian law is not suited to analyze the line shape of the diffuse ring in the powder diffraction pattern of the SmI phase of TBDA.

Powder samples

The powder patterns were recorded with a high-resolution Guinier camera equipped with an electric heating stage and using a focused monochromatic beam [$\lambda(\mathrm{Co}\,K\alpha_1) = 1.7889$ Å]. The sample is placed on a grating which oscillates in its plane and as all orientations are statistically represented any effect of mosaic spread of a given single domain is canceled. The intensity profiles obtained for the SmF and SmI phases of TBDA are shown in Figs. 4–6.

In order to analyze these profiles we assume that the layers are uncorrelated so that the intensity scattered from all the layers is proportional to that scattered by a single layer. The partial structure in the c^* direction $G(q_z)$ is derived from the square of the Fourier transform of the molecular electron density ρ. This is described to a very good approximation as the sum of two step functions characteristic of the core and of the end chains.[11]

The total structure factor must take into account the order within the layers which is characterized by $f_{\vec G}(q_x, q_y)$ (Fig. 1). The total structure factor is, then, the product of the structure factor along c^* and the in-plane structure factor $S(\vec q) \propto f_{\vec G}(q_x, q_y)\cdot g(q_z)$, where q_x, q_y are the in-plane components, and q_z is the c^* component of $\vec q$.

The main characteristic of a powder diagram is that all the orientations of the sample are statistically represented which implies that the intensity distribution $I_{\vec G}(\vec Q)$ ($\vec Q$ is the scattering vector) is obtained by summing the intensity located around an $hk0$ point of the reciprocal lattice over a sphere centered at the origin of the reciprocal space and whose radius is Q. The intensity is formally written as

$$I_{\vec G}(\vec Q) = \int d^3k\, S(\vec k)\, \delta(|\vec k|^2 - |\vec Q|^2),$$

where $\vec G = ha^* + kb^*$ and $\vec k = \vec G + \vec q$.

In the SmF phase of TBPA (Ref. 11) it has been shown that the diffuse ring can be analyzed with a Lorentzian in-plane structure factor characteristic of a short-range positional order and we find again the same law in the SmF phase of TBDA:

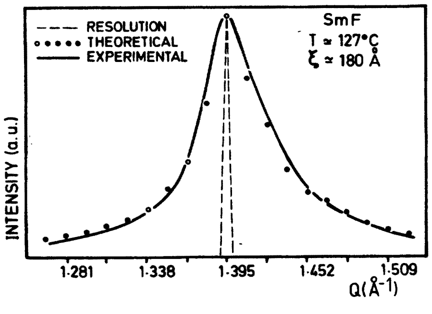

FIG. 4. Comparison of the line shape of the diffuse ring in the powder diffraction pattern for the SmF phase of TBDA with the calculated curve using the Lorentzian law for $f(q_x, q_y)$ (see text).

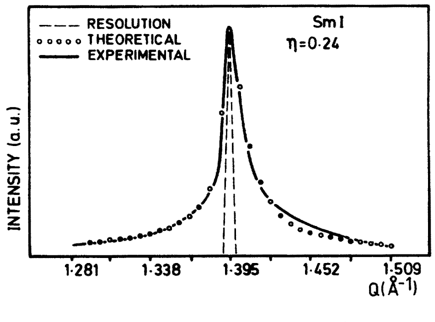

FIG. 6. Comparison of the line shape for the SmI phase of TBDA with the calculated curve using a correlation function with power-law decay (see text).

$$f_{\vec{G}}(q_x, q_y) \sim [\xi^2(q_x^2+q_y^2)+1]^{-1}$$

defining a correlation length

$$\xi = 180 \pm 20\ \text{Å at } T \sim 127\,^\circ\text{C}\ .$$

Figure 4 displays an example of a fit of the experimental line shape.

At lower temperatures the correlation length increases: at $T\sim 120\,^\circ\text{C}$, $\xi = 250 \pm 30$ Å. It appears therefore that whatever the homolog, ξ has the same order of magnitude but never diverges.

The main difference in the powder patterns between SmF and SmI is that the half-width of the $hk0$ ring for the latter is approximately four times narrower. Therefore, the SmI phase appears very much better ordered than the SmF phase although it appears at a higher temperature.

Taking into account the different orientation of the tilt angle, for the SmI phase, we have tried to analyze the experimental line shape using, as for the SmF phase, a Lorentzian structure factor, but such law does not give good agreement with the experimental data as can be seen in Fig. 5. We have therefore used a power-law decay to characterize the positional order:

$$f_{\vec{G}}(q_x, q_y) \propto (q_x^2+q_y^2)^{(-2+\eta)/2}\ .$$

This law brings the "sidebands" of the line shape up and permits good agreement with the experimental scattering factor (Fig. 6). Meanwhile as this law diverges, one has to perform the convolution of the structure factor with the resolution function of the spectrometer. Except in a range of less than ± 0.01 Å^{-1} around the maximum of the curve, our resolution function, whose width is small compared with the observed phenomena, has no drastic effects. At $T\sim 152\,^\circ\text{C}$ we find $\eta = 0.24 \pm 0.02$. A temperature dependence of η has not been observed since the variation of η would not be significant in the temperature range of existence of the SmI phase ($\lesssim 8\,^\circ\text{C}$). The homolog C_{15} with a larger temperature range of stability might allow such an analysis.

DISCUSSION

The behavior of the SmF, but not the SmI, phase may readily be understood in terms of the theory of 2D melting proposed by Halperin and Nelson[12] following the work of Kosterlitz and Thouless.[13] At low temperatures a 2D phase is expected to show long-range bond orientational order and quasi-long-range positional order with a positional correlation function decaying algebraically like $r^{-\eta(T)}$, giving rise to power-law singularities in the scattering in place of true Bragg reflections. At sufficiently high temperatures melting occurs by the dissociation of a small fraction of bound dislocation pairs to give the hexatic phase which has quasi-long-range bond orientational order (algebraic decay) but short-range positional correlations of the form $\exp(-r/\xi)$, where ξ is the correlation length, which is readily obtained from the Lorentzian scattering profile $(\xi^2|\vec{Q}-\vec{G}|^2+1)^{-1}$. In this phase the orientational defects which are the disclinations form bound pairs and a second disclination unbinding transition is necessary to complete the transition from solid to liquid.

The algebraic decay of correlation functions is associated with an infinite corresponding susceptibility so that weak interlayer coupling, as in certain smectic liquid crystals, would convert the above partially ordered 2D phases into either a true crystal phase or a hexatic phase with long-range bond orientational order.[14] The latter behavior is now established in SmF and SmB phases with $\xi\sim 100$ Å, compared with $\xi \sim 10$ Å for the true liquidlike layers of SmA or SmC phases. We have shown here that insofar as it possesses algebraic decay of positional correlations the SmI phase appears to behave like an *uncoupled* 2D crystalline phase. Still more surprisingly, however, where the SmF and SmI phases occur in the same compound the SmI is the higher temperature phase and no theory currently exists to explain a phase transition which produces longer-range positional correlation with increasing temperature. This situation is not, however, unique as $5O\cdot 6$ (Ref. 7) (see Table I) has an SmF phase appearing between crystalline SmG and SmB phases as the temperature is increased.

In conclusion, we have confirmed in TBDA that the SmF phase has a stacked tilted hexatic structure (long-range bond orientational order but short-range positional order) and have established that the SmI phase is a quasi-two-dimensional phase (no positional correlation between layers) with algebraic decay of positional correlation within layers. The SmI phase has previously been shown to have long-range bond orientational order. The SmI and SmF phases also differ in the direction of the molecular tilt relative to the hexagonal molecular packing but no relationship is yet apparent between this and the type of correlation. The type of order in SmI and its relationship to SmF both appear to be anomalous.

ACKNOWLEDGMENT

We thank S.R.C. for financial support and A. M. Levelut and P. G. Wrighton for useful discussions.

[1] J. D. Litster, in *Liquid Crystals of One- and Two-Dimensional Order*, edited by W. Helfrich and G. Hepple (Springer, Berlin, 1980), p. 65.

[2] P. A. C. Gane, A. J. Leadbetter, and P. G. Wrighton, Mol. Cryst. Liq. Cryst. 66, 247 (1981); J. J. Benattar, F. Moussa, and M. Lambert, J. Phys. (Paris) Lett. 42, L67 (1981).

[3] R. Pindak, D. E. Moncton, S. C. Davey, and J. W. Goodby, Phys. Rev. Lett. (to be published).

[4] A. J. Leadbetter, J. P. Gaughan, B. Kelly, G. W. Gray, and J. W. Goodby, J. Phys. (Paris) 40, C3–178 (1979); J. J. Benattar, J. Doucet, M. Lambert, and A. M. Levelut, Phys. Rev. A 20, 2505 (1979).

[5] S. Diele, D. Demus, and H. Sackmann, Mol. Cryst. Liq. Cryst. Lett. 56, 217 (1980).

[6] A. J. Leadbetter, M. A. Mazid, and R. M. Richardson, in *Liquid Crystals*, edited by S. Chandrasekhar (Heydon, London, 1980), p. 65.

[7] J. W. Goodby, G. W. Gray, A. J. Leadbetter, and M. A. Mazid, J. Phys. (Paris) 41, 591 (1980).

[8] E. M. Barrall II, J. W. Goodby, and G. W. Gray, Mol. Cryst. Liq. Cryst. Lett. 49, 319 (1979).

[9] P. A. C. Gane, A. J. Leadbetter, P. G. Wrighton, J. W. Goodby, and G. W. Gray (unpublished).

[10] J. Doucet, P. Keller, A. M. Levelut, and P. Porguet, J. Phys. (Paris) 39, 548 (1978).

[11] J. J. Benattar, F. Moussa, and M. Lambert, J. Phys. (Paris) 41, 1371 (1980).

[12] B. I. Halperin and D. R. Nelson, Phys. Rev. Lett. 41, 121 (1978); D. R. Nelson and B. I. Halperin, Phys. Rev. B 19, 2457 (1979).

[13] J. M. Kosterlitz and D. J. Thouless, J. Phys. C 6, 1181 (1973).

[14] R. J. Birgeneau and J. D. Lister, J. Phys. (Paris) Lett. 39, L399 (1978).